Supporting information for:

Large scale in silico screening of materials for carbon capture through chemical looping

Cindy Y. Lau,[†,¶] Matthew T. Dunstan,[‡,¶] Wenting Hu,[†] Clare P. Grey,[*,‡] and Stuart A. Scott[*,†]

†*Department of Engineering, University of Cambridge, Trumpington Street, Cambridge, CB2 1PZ, United Kingdom*

‡*Department of Chemistry, University of Cambridge, Lensfield Road, Cambridge, CB2 1EW, United Kingdom*

¶*Contributed equally to this work*

E-mail: cpg27@cam.ac.uk; sas37@cam.ac.uk

Candidate sample masses for TGA experiments

The sample masses for the initial TGA characterisation for the candidate materials are shown in Table S1.

Table S1: Masses of the candidate materials used in the TGA experiments.

Compound	Sample mass (mg)
$SrFeO_3$	15.8
$BaFeO_3$	23.5
$BaBiO_3$	25.0
$BaCoO_3$	27.9

Candidate materials obtained from the screening

The 108 materials obtained after restricting the screening results to those involving only single oxide to oxide reactions, containing relatively safe and abundant elements, are summarised in Table S2. Materials that are particularly interesting due to their oxygen capacity or $T_{reduction}$ at $p_{O_2} = 0.21$ bar are shown in bold.

Table S2: Theoretically derived reduction reaction parameters for the candidates obtained from the screening, restricted to single oxide to oxide reactions from relatively safe and abundant elements.

Compound	$\Delta H_{reduction}$	O_2 capacity	$T_{reduction}$	Reaction
	kJ mol^{-1}	$g_{O_2}/g_{sorbent}$	K	
Ta_2O_5	39.4	0.543	207	$0.133\,Ta_2O_5 + O_2 \longrightarrow 0.267\,TaO_{10}$
BaH_4O_3	43.4	0.253	226	$0.667\,BaH_4O_3 + O_2 \longrightarrow 0.667\,Ba(H_2O_3)_2$
SeO_2	46.9	0.072	242	$4\,SeO_2 + O_2 \longrightarrow 2\,Se_2O_5$
$Cu_2P_2O_7$	50.9	0.053	259	$2\,Cu_2P_2O_7{}^{+}O_2 \longrightarrow 4\,CuPO_4$
Bi_4O_7	52.8	0.017	268	$2\,Bi_4O_7{}^{+}O_2 \longrightarrow 8\,BiO_2$

Pr_2O_3	54.3	0.029	275	$3.333\,Pr_2O_3 + O_2 \longrightarrow 1.333\,Pr_5O_9$
$Ba(HO)_2$	59.5	0.187	298	$Ba(OH)_2 + O_2 \longrightarrow Ba(HO_2)_2$
K_2O_2	66.2	0.290	327	$K_2O_2 + O_2 \longrightarrow 2\,KO_2$
Na_2O	69.3	0.774	341	$0.667\,Na_2O + O_2 \longrightarrow 1.333\,NaO_2$
CuO	70.0	0.101	343	$4\,CuO + O_2 \longrightarrow 2\,Cu_2O_3$
$NaMnO_2$	70.1	0.291	344	$NaMnO_2 + O_2 \longrightarrow NaMnO_4$
Li_2O	74.8	0.535	364	$2\,Li_2O + O_2 \longrightarrow 2\,Li_2O_2$
SrO	83.8	0.154	402	$2\,SrO + O_2 \longrightarrow 2\,SrO_2$
$Mn(PO_3)_2$	84.1	0.075	404	$2\,Mn(PO_3)_2 + O_2 \longrightarrow 2\,MnP_2O_7$
Cs_2O_2	86.7	0.107	415	$Cs_2O_2 + O_2 \longrightarrow 2\,CsO_2$
$CaSe_2O_5$	87.8	0.058	419	$2\,CaSe_2O_5 + O_2 \longrightarrow 2\,Ca(SeO_3)_2$
Nd_2O_3	92.7	0.095	440	$Nd_2O_3 + O_2 \longrightarrow Nd_2O_5$
SiO_2	94.2	0.044	446	$12\,SiO_2 + O_2 \longrightarrow 2\,Si_6O_{13}$
YbO	97.9	0.085	461	$2\,YbO + O_2 \longrightarrow 2\,YbO_2$
$Sr_8Fe_8O_{23}$	104.4	0.011	488	$2\,Sr_8Fe_8O_{23} + O_2 \longrightarrow 16\,SrFeO_3$
MoP_2O_7	108.2	0.059	503	$2\,MoP_2O_7 + O_2 \longrightarrow 2\,Mo(PO_4)_2$
$Ce(SeO_3)_2$	108.7	0.081	505	$Ce(SeO_3)_2 + O_2 \longrightarrow Ce(SeO_4)_2$
Bi_2O_3	110.6	0.034	513	$2\,Bi_2O_3 + O_2 \longrightarrow 4\,BiO_2$
$Ba_4Fe_4O_{11}$	115.1	0.017	531	$2\,Ba_4Fe_4O_{11} + O_2 \longrightarrow 8\,BaFeO_3$
$ZnSeO_3$	124.6	0.083	570	$2\,ZnSeO_3 + O_2 \longrightarrow 2\,ZnSeO_4$
K_2O	134.9	0.510	611	$0.667\,K_2O + O_2 \longrightarrow 1.333\,KO_2$
$EuMnO_3$	136.1	0.031	616	$4\,EuMnO_3 + O_2 \longrightarrow 2\,Eu_2Mn_2O_7$
$YbVO_3$	136.3	0.029	616	$4\,YbVO_3 + O_2 \longrightarrow 2\,Yb_2V_2O_7$
$Mn_3Se_3O_{10}$	137.1	0.057	620	$Mn_3Se_3O_{10} + O_2 \longrightarrow 3\,MnSeO_4$
CoO	137.3	0.214	621	$2\,CoO + O_2 \longrightarrow 2\,CoO_2$
VSO_5	139.1	0.049	628	$4\,VSO_5 + O_2 \longrightarrow 2V_2S_2O_{11}$
Mn_2O_3	141.0	0.101	635	$2\,Mn_2O_3 + O_2 \longrightarrow 4\,MnO_2$

$NiSeO_3$	142.8	0.086	642	$2\,NiSeO_3 + O_2 \longrightarrow 2\,NiSeO_4$
Cs_2O	143.5	0.170	645	$0.667\,Cs_2O + O_2 \longrightarrow 1.333\,CsO_2$
$Sc_2(SeO_3)_3$	156.0	0.102	694	$0.667\,Sc_2(SeO_3)_3 + O_2 \longrightarrow 0.667\,Sc_2(SeO_4)_3$
BaO	161.4	0.104	715	$2\,BaO + O_2 \longrightarrow 2\,BaO_2$
$\mathbf{LiBiO_2}$	162.1	0.065	718	$2\,LiBiO_2 + O_2 \longrightarrow 2\,LiBiO_3$
$MnSe_2O_5$	163.3	0.055	723	$2\,MnSe_2O_5 + O_2 \longrightarrow 2\,Mn(SeO_3)_2$
$\mathbf{SrCuO_2}$	164.6	0.044	728	$4\,SrCuO_2 + O_2 \longrightarrow 2\,Sr_2Cu_2O_5$
$\mathbf{Sr_2Fe_2O_5}$	168.2	0.044	742	$2\,Sr_2Fe_2O_5 + O_2 \longrightarrow 4\,SrFeO_3$
Rb_2O_3	168.8	0.219	744	$0.667\,Rb_2O_3 + O_2 \longrightarrow 1.333\,RbO_3$
$\mathbf{Mn_2P_2O_7}$	169.0	0.056	745	$2\,Mn_2P_2O_7 + O_2 \longrightarrow 4\,MnPO_4$
$Ho_2(SeO_3)_3$	172.0	0.068	756	$0.667\,Ho_2(SeO_3)_3 + O_2 \longrightarrow 0.667\,Ho_2(SeO_4)_3$
V_3O_7	177.1	0.030	776	$4\,V_3O_7 + O_2 \longrightarrow 6\,V_2O_5$
Ti_3O_5	178.2	0.394	780	$0.364\,Ti_3O_5 + O_2 \longrightarrow 0.545\,Ti_2O_7$
Mn_3O_4	178.6	0.140	782	$Mn_3O_4 + O_2 \longrightarrow 3\,MnO_2$
$\mathbf{Ba_2Fe_2O_5}$	188.8	0.034	821	$2\,Ba_2Fe_2O_5 + O_2 \longrightarrow 4\,BaFeO_3$
$CoSeO_3$	190.0	0.086	825	$2\,CoSeO_3 + O_2 \longrightarrow 2\,CoSeO_4$
Cs_3O	192.7	0.193	836	$0.4\,Cs_3O + O_2 \longrightarrow 1.2\,CsO_2$
$\mathbf{KBiO_2}$	193.2	0.057	838	$2\,KBiO_2 + O_2 \longrightarrow 2\,KBiO_3$
$MoPO_5$	197.9	0.039	856	$4\,MoPO_5 + O_2 \longrightarrow 2\,Mo_2P_2O_{11}$
$MnSeO_3$	198.0	0.088	856	$2\,MnSeO_3 + O_2 \longrightarrow 2\,MnSeO_4$
$Na_2Mn_2O_3$	200.4	0.392	865	$0.4\,Na_2Mn_2O_3 + O_2 \longrightarrow 0.8\,NaMnO_4$
$SmMnO_3$	200.5	0.032	865	$4\,SmMnO_3 + O_2 \longrightarrow 2\,Sm_2Mn_2O_7$
$\mathbf{NaBiO_2}$	205.6	0.061	885	$2\,NaBiO_2 + O_2 \longrightarrow 2\,NaBiO_3$
$TlPO_3$	210.3	0.056	902	$2\,TlPO_3 + O_2 \longrightarrow 2\,TlPO_4$
$Cs_{11}O_3$	211.7	0.201	908	$0.105\,Cs_{11}O_3 + O_2 \longrightarrow 1.158\,CsO_2$
$Mo_2(PO_4)_3$	212.8	0.034	912	$2\,Mo_2(PO_4)_3 + O_2 \longrightarrow 2\,Mo_2P_3O_{13}$
$MgSeO_3$	213.9	0.106	916	$2\,MgSeO_3 + O_2 \longrightarrow 2\,MgSeO_4$

Cu_2O	215.0	0.224	920	$Cu_2O + O_2 \longrightarrow Cu_2O_3$
$LuMnO_3$	227.2	0.029	966	$4\,LuMnO_3 + O_2 \longrightarrow 2\,Lu_2Mn_2O_7$
Rb_2O	229.4	0.428	974	$0.4\,Rb_2O + O_2 \longrightarrow 0.8\,RbO_3$
$TmMnO_3$	231.5	0.029	982	$4\,TmMnO_3 + O_2 \longrightarrow 2\,Tm_2Mn_2O_7$
$ErMnO_3$	233.2	0.030	988	$4\,ErMnO_3 + O_2 \longrightarrow 2\,Er_2Mn_2O_7$
VO_2	233.6	0.096	989	$4\,VO_2 + O_2 \longrightarrow 2\,V_2O_5$
$DyMnO_3$	233.7	0.030	990	$4\,DyMnO_3 + O_2 \longrightarrow 2\,Dy_2Mn_2O_7$
$HoMnO_3$	234.2	0.030	992	$4\,HoMnO_3 + O_2 \longrightarrow 2\,Ho_2Mn_2O_7$
$YMnO_3$	236.6	0.042	1001	$4\,YMnO_3 + O_2 \longrightarrow 2\,Y_2Mn_2O_7$
Ti_2O_3	237.2	0.445	1003	$0.5\,Ti_2O_3 + O_2 \longrightarrow 0.5\,Ti_2O_7$
SbO_2	237.8	0.052	1005	$4\,SbO_2 + O_2 \longrightarrow 2Sb_2O_5$
Cs_7O	249.1	0.220	1047	$0.154\,Cs_7O + O_2 \longrightarrow 1.077\,CsO_2$
P_2WO_7	249.7	0.045	1049	$2\,P_2WO_7 + O_2 \longrightarrow 2\,P_2WO_8$
$SrSeO_3$	259.6	0.075	1085	$2\,SrSeO_3 + O_2 \longrightarrow 2\,SrSeO_4$
PWO_5	263.1	0.027	1099	$4\,PWO_5 + O_2 \longrightarrow 2\,P_2W_2O_{11}$
$TbMnO_3$	263.5	0.031	1100	$4\,TbMnO_3 + O_2 \longrightarrow 2\,Tb_2Mn_2O_7$
$BaSeO_3$	263.7	0.061	1101	$2\,BaSeO_3 + O_2 \longrightarrow 2\,BaSeO_4$
VPO_4	264.8	0.110	1105	$2\,VPO_4 + O_2 \longrightarrow 2\,VPO_5$
$LaCuO_2$	266.1	0.068	1109	$2\,LaCuO_2 + O_2 \longrightarrow 2\,LaCuO_3$
Li_3BiO_3	267.5	0.058	1114	$2\,Li_3BiO_3 + O_2 \longrightarrow 2\,Li_3BiO_4$
Rb_9O_2	269.2	0.499	1121	$0.08\,Rb_9O_2 + O_2 \longrightarrow 0.72\,RbO_3$
$EuSeO_3$	270.1	0.057	1124	$2\,EuSeO_3 + O_2 \longrightarrow 2\,EuSeO_4$
$SmCuO_2$	275.5	0.065	1144	$2\,SmCuO_2 + O_2 \longrightarrow 2\,SmCuO_3$
MnO	276.1	0.226	1146	$2\,MnO + O_2 \longrightarrow 2\,MnO_2$
Rb_6O	278.0	0.514	1153	$0.118Rb_6O + O_2 \longrightarrow 0.706\,RbO_3$
K_4I_2O	278.8	0.300	1156	$0.25K_4I_2O + O_2 \longrightarrow 0.25\,K_4I_2O_9$
$\mathbf{Sr_2Bi_2O_5}$	280.4	0.024	1162	$2\,Sr_2Bi_2O_5 + O_2 \longrightarrow 4\,SrBiO_3$

Na_2SeO_3	289.1	0.093	1193	$2\,Na_2SeO_3 + O_2 \longrightarrow 2\,Na_2SeO_4$
LiCuO	290.7	0.185	1199	$2\,LiCuO + O_2 \longrightarrow 2\,LiCuO_2$
VBO_3	293.2	0.146	1208	$2\,VBO_3 + O_2 \longrightarrow 2\,VBO_4$
Tl_4O_3	293.2	0.055	1208	$0.667\,Tl_4O_3 + O_2 \longrightarrow 1.333\,Tl_2O_3$
Mo_8O_{23}	297.2	0.014	1223	$2\,Mo_8O_{23} + O_2 \longrightarrow 16\,MoO_3$
Tl_2O	301.1	0.075	1236	$Tl_2O + O_2 \longrightarrow Tl_2O_3$
V_3O_5	309.5	0.172	1267	$0.8\,V_3O_5 + O_2 \longrightarrow 1.2\,V_2O_5$
MoO_2	317.0	0.125	1294	$2\,MoO_2 + O_2 \longrightarrow 2\,MoO_3$
$Mo_2P_3O_{11}$	325.7	0.069	1325	$Mo_2P_3O_{11} + O_2 \longrightarrow Mo_2P_3O_{13}$
$SbPO_4$	326.7	0.074	1328	$2\,SbPO_4 + O_2 \longrightarrow 2\,SbPO_5$
K_3IO	329.2	0.246	1337	$0.5\,K_3IO + O_2 \longrightarrow 0.5\,K_3IO_5$
NaCuO	332.3	0.156	1348	$2\,NaCuO + O_2 \longrightarrow 2\,NaCuO_2$
V_2O_3	334.4	0.214	1356	$V_2O_3 + O_2 \longrightarrow V_2O_5$
$\mathbf{Sr_2Mn_2O_5}$	339.6	0.044	1374	$2\,Sr_2Mn_2O_5 + O_2 \longrightarrow 4\,SrMnO_3$
Sb_2O_3	340.2	0.110	1376	$Sb_2O_3 + O_2 \longrightarrow Sb_2O_5$
$\mathbf{Ba_2Bi_2O_5}$	342.0	0.021	1383	$2\,Ba_2Bi_2O_5 + O_2 \longrightarrow 4\,BaBiO_3$
Na_3BiO_3	346.5	0.049	1399	$2\,Na_3BiO_3 + O_2 \longrightarrow 2\,Na_3BiO_4$
$MgVO_3$	346.9	0.065	1400	$4\,MgVO_3 + O_2 \longrightarrow 2\,Mg_2V_2O_7$
CsCuO	354.0	0.075	1425	$2\,CsCuO + O_2 \longrightarrow 2\,CsCuO_2$
KCuO	356.7	0.135	1435	$2\,KCuO + O_2 \longrightarrow 2\,KCuO_2$
$\mathbf{BaCoO_2}$	359.3	0.070	1444	$2\,BaCoO_2 + O_2 \longrightarrow 2\,BaCoO_3$
$NaNO_2$	373.4	0.232	1494	$2\,NaNO_2 + O_2 \longrightarrow 2\,NaNO_3$

Effect of heating rate on TGA experiments

Figure S1 shows the mass as a function of time and temperature for cycles of heating and cooling in the TGA with air injected through the reaction gas port. Owing to mixing in the TGA the actual concentration of oxygen at the surface of the sample would be approximately 1.5×10^4 Pa. The mass change of the sample is small so some influence due to the slight drift in the balance can be observed. However, it can be seen that the mass of sample at a given temperature is largely independent of the heating rate used on heating, and the mass rise on cooling at 20 K min^{-1} follows the mass loss on heating at different heating rates, with little hysteresis. This indicates that the sample is coming to equilibrium with the instantaneous temperature and local partial pressure and that in this experiment there is little lag, with all heating rates showing similar mass vs sample temperature curves on heating. The exception is perhaps the heating rate at 20 K min^{-1} per minute in these particular experiments, which shows a small amount of hysteresis. However, when a higher sample mass was used, as in the original data presented in Figure 3 of the manuscript (where the initial mass of sample was 15.8 mg), such hysteresis was not observed.

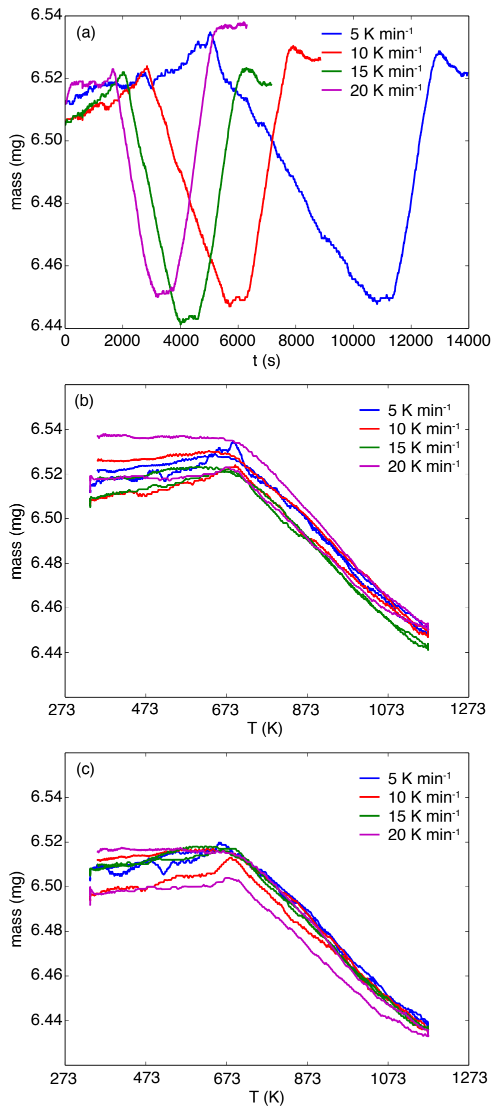

Figure S1: TGA traces for $SrFeO_{3-\delta}$, subjected to heating rates of 5, 10, 15 and 20 K min^{-1} to 1173 K and then cooled to 50 K at 20 K min^{-1}. (a) and (b) second set of cycles, (c) third set of cycles. The cycles within a set were carried out in a random order.

Microstructure of $SrFeO_{3-\delta}$

Secondary and backscattered electron micrographs were collected using a field emission gun scanning electron microscope (Zeiss) operating at an accelerating voltage of 2.4 kV. SEM images of the as-prepared $SrFeO_{3-\delta}$ sample are shown in Figure S2. As expected from a close packed oxide material, there is negligible porosity or surface area observed in the sample.

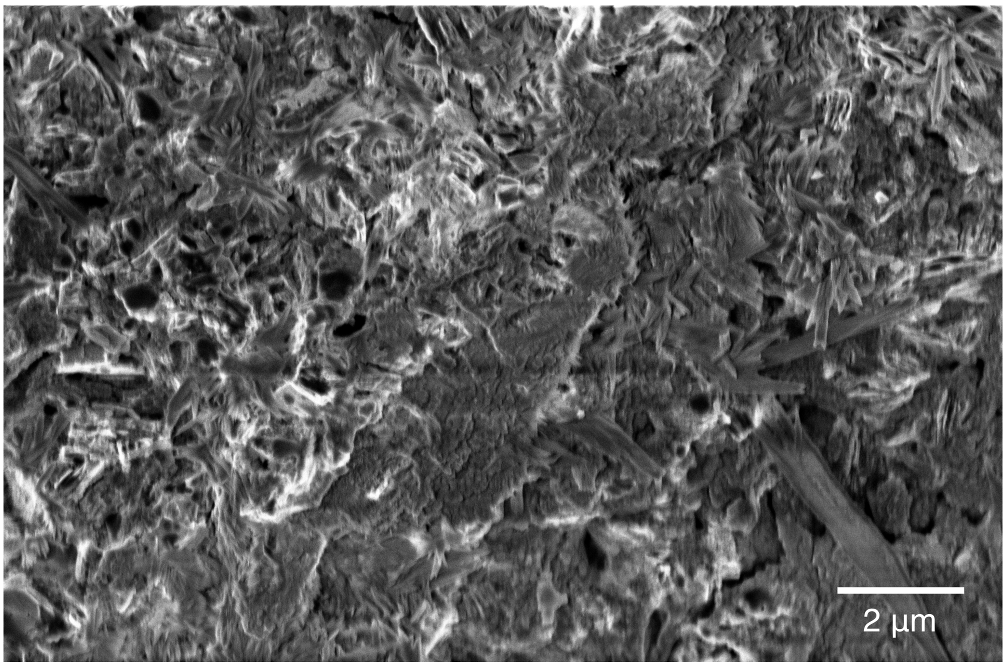

Figure S2: SEM images of the $SrFeO_{3-\delta}$ sample.

XRD of reduced candidate phases

XRD diffractograms of the as-prepared samples of $BaBiO_3$ and $BaCoO_3$, as well as the samples after reduction under N_2, are shown in Figure S3. In both cases, the reduction reactions proceed as predicted by the Materials Project, to $Ba_2Bi_2O_5$ and $BaCoO_2$ respectively.

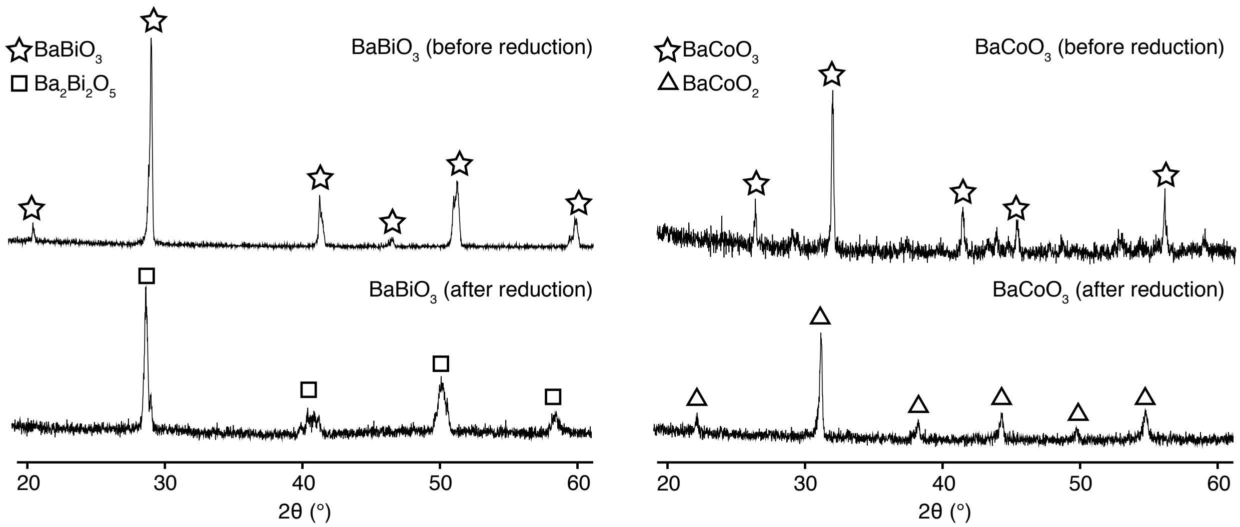

Figure S3: XRD diffractograms (λ=1.5405 Å) for $BaBiO_3$ and $BaCoO_3$, both before and after reduction. In both cases, the phases remaining after reduction, Ba_2BiO_5 and $BaCoO_2$ respectively, match the predicted reduction reaction from the Materials Project.

Oxygen content of $SrFeO_{3-\delta}$

TGA experiments were performed on the as-synthesised $SrFeO_{3-\delta}$ sample (17 mg) under reducing 5% H_2 in N_2 gas flow to determine the oxygen content, the result of which is shown in Figure S4. The sample was removed after the first significant mass loss, corresponding to complete reduction to $SrFeO_{2.5}$. Subsequent XRD of the retrieved sample confirmed this full reduction to the brownmillerite phase. From the measured mass loss corresponding to this transition, the initial stiochiometry of the phase was determined to be $SrFeO_{2.78}$. The additional reduction in mass upon further heated is attributed to further reduction of the brownmillerite phase (which is only possible under such strongly reducing conditions used here).

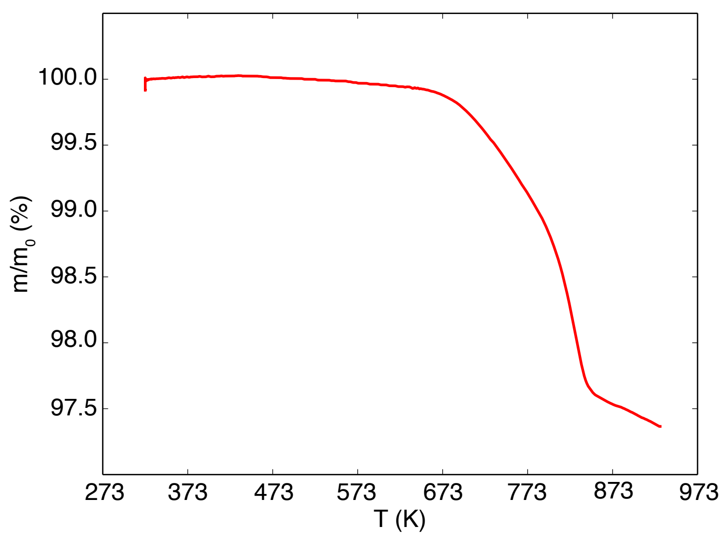

Figure S4: Temperature programmed reduction of $SrFeO_{3-\delta}$ sample in the TGA. The sample was first heated in air, cooled and subjected to a cycle of heating and cooling at 20 K min^{-1} to 1173 K. The experiment was terminated after the first significant mass loss, corresponding to complete reduction to $SrFeO_{2.5}$.

Isothermal pressure swing studies of $SrFeO_{3-\delta}$

TGA traces during isothermal pressure swing are shown in Figure S5, with all masses are normalised on the mass of the most oxidised sample in air at 473 K.

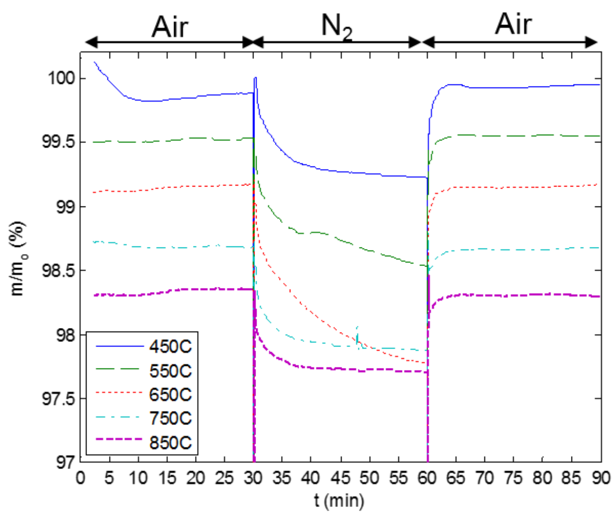

Figure S5: Isothermal pressure swing TGA traces with all masses normalised on the mass of the most oxidised sample in air at low temperature (473 K). Pressure swing of sample with pure $SrFeO_{3-\delta}$ in TGA for consecutive cycles of 30 min air - 30 min N_2 - 30 min air from 723 K to 1123 K.